Ordering and Excitations in the Field-Induced Magnetic Phase of $Cs_3Cr_2Br_9$

B. Grenier,[1] Y. Inagaki,[2] L. P. Regnault,[1] A. Wildes,[3] T. Asano,[2] Y. Ajiro,[2] E. Lhotel,[4] C. Paulsen,[4] T. Ziman,[3] and J. P. Boucher[5]

[1]*Département de Recherche Fondamentale sur la Matière Condensée, SPSMS, Laboratoire Magnétisme et Diffraction Neutronique, CEA-Grenoble, 38054 Grenoble cedex 9, France*

[2]*Department of Physics, Kyushu University, Fukuoka 850-8581, Japan*

[3]*Institut Laue Langevin, BP 156, 38042 Grenoble cedex 9, France*

[4]*Centre de Recherches sur les Très Basses Températures CNRS, BP 166, 38042 Grenoble cedex 9, France*

[5]*Laboratoire de Spectrométrie Physique, Université J. Fourier, BP 87, 38402 Saint Martin d'Hères, France*

(Received 17 July 2003; published 30 April 2004)

Field-induced magnetic order has been investigated in detail in the interacting spin 3/2 dimer system $Cs_3Cr_2Br_9$. Elastic and inelastic neutron scattering measurements were performed up to $H = 6$ T, well above the critical field $H_{c1} \sim 1.5$ T. The ordering displays incommensurabilities and a large hysteresis before a commensurate structure is reached. This structure is fully determined. Surprisingly, the lowest excitation branch never closes. Above H_{c1}, the gap increases slowly with the field. An analysis in terms of projected pseudospins is given.

DOI: 10.1103/PhysRevLett.92.177202 PACS numbers: 75.10.Jm, 75.40.Gb, 78.70.Nx

In recent years, a great deal of work has been devoted to isotropic quantum spin systems which show a gap in their energy spectrum. This includes a large variety of different models such as Haldane and alternating chains, ladders, as well as spin-dimer systems. In a zero magnetic field, these systems are all characterized by an $S = 0$ singlet ground state ($|0\rangle$) and the energy gap E_G of the lowest magnetic excitation corresponds to an $S = 1$ state ($|1\rangle$). In a field H, when the gap closes at $H = H_{c1}$ ($g\mu_B H_{c1} \sim E_G$) a three-dimensional magnetic ordering develops, induced by the small interchain and/or interdimer couplings. In these field-induced magnetic orderings (FIMO) only the spin components transverse to the applied field spontaneously break symmetry. Moreover, as initially proposed for Haldane chains, a FIMO transition is an experimental realization of a Bose-Einstein condensation (BEC) of the hard-sphere bosons, the magnons, into the ground state [1]. Recently, the magnetic behavior observed in the $s = \frac{1}{2}$ spin-dimer compound $TlCuCl_3$ has been analyzed within this framework [2,3]. While for BEC a gapless Goldstone mode is present in the energy spectrum of the condensed phase, in the case of a FIMO, the mode is gapless only if there is conservation of the component of the total spin in the field direction. If this symmetry is broken, the total number of the magnons is no longer conserved. A gap may then be seen in the lowest excitation branch. It is important to understand the way an anisotropy creates such a gap in a FIMO phase. In this Letter we present a complementary elastic and inelastic neutron investigation of the FIMO phase in the spin-dimer system $Cs_3Cr_2Br_9$. This material differs from $TlCuCl_3$ and similar compounds [4] in two significant respects. The larger spin value of Cr^{3+}, $s = 3/2$ favors the presence of local anisotropies. The crystal structure is different: the spin dimers form a hexagonal arrangement in the (**a**, **b**) plane as shown in Fig. 1. This leads to frustration, which should strongly affect any magnetic order. These two points, i.e., the role of a small anisotropy and the effects of frustration in a FIMO, are demonstrated here experimentally. An analysis in terms of projected pseudospins is proposed to discuss the striking features in the magnetic phase.

The spin-excitation spectrum of $Cs_3Cr_2Br_9$ in a zero field was determined across the whole Brillouin zone by Leuenberger *et al.* [5]. The intra- and interdimer exchange couplings are all *antiferromagnetic* (AFM). In a field, Zeeman splitting was also observed, but only for small fields, $H \leq H_{c1}$ [6]. Neither the field-induced magnetic structure nor the field dependence of the spin excitations has been studied above H_{c1}. Here, we investigate this FIMO phase in detail. Our experimental configuration is the same as in Ref. [6]: the external field H is applied

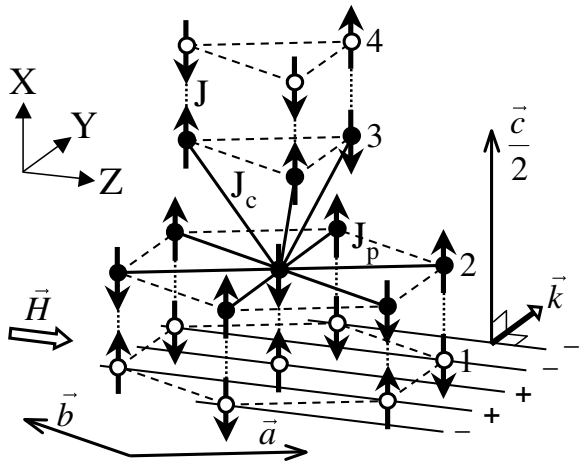

FIG. 1. Transverse spin order of the Cr^{3+} ions in the commensurate $++--$ magnetic phase of $Cs_3Cr_2Br_9$ for $\mathbf{H} \parallel \mathbf{a} - \mathbf{b}$. $\mathbf{k}$ is the propagation vector of the magnetic order.

within the (**a**, **b**) plane along the **a** − **b** axis (hereafter defined as the Z axis) so that the XY plane where the AFM ordered moments are expected to lie (*transverse ordering*) is defined by the **c** (hereafter X) and the **a** + **b** (Y) axes (Fig. 1). $Cs_3Cr_2Br_9$ crystallizes in the hexagonal $P6_3/mmc$ structure, with $a = b = 7.508$ Å, $c = 18.70$ Å (which is twice the distance between successive planes), and consists of four Bravais sublattices. The $s = 3/2$ Cr^{3+} dimers lie parallel to the **c** axis [8].

First, we present the elastic results. They were performed on the lifting-arm two-axis diffractometer D23 CEA-CRG at the Institut Laue-Langevin (ILL) in Grenoble, France. A single crystal ($\sim$350 mm^3) of $Cs_3Cr_2Br_9$ was placed in a 6 T vertical cryomagnet equipped with a dilution insert. The wavelength was $\lambda =$ 1.28 Å and the temperature was maintained in the range 50–100 mK. In a zero field, 113 nuclear reflections were collected, which could be reduced to 68 independent measurements. The structural refinement was achieved with type II Becker-Coppens Gaussian extinction correction and isotropic thermal factors. A weighted R factor of 1.7% on the nuclear structure factors F_N was obtained by refining 12 parameters. The magnetic structure was then determined at $H = 6$ T. It is described by the commensurate propagation wave vector $\mathbf{k} = (1/4, 1/4, 0)$ [9]. Because of the symmetry, two other magnetic domains were observed, corresponding to the wave vectors $(1/4, -1/2, 0)$, $(-1/2, 1/4, 0)$. One hundred twenty-three magnetic reflections were collected in the three domains. For the magnetic refinement an isotropic Cr^{3+} magnetic form factor was used, yielding a weighted R factor of 4.2% on the magnetic structure factors F_M. This gives (i) that the populations of the three domains are about the same (34.8 ± 0.6, 33.0 ± 0.4, and 32.2 ± 0.4%) and the magnetic structure is collinear with the moments pointing along the **c** ($\equiv X$) direction; this agrees with the expected transverse ordering for a FIMO. (ii) The arrangement of the transverse magnetic moments within one cell is represented in Fig. 1 (atoms labeled 1, 2, 3, 4). If we assume the moment amplitude to be constant (as is usual for 3d ions), this motif propagates with the sequence $++--$ along the (110) direction (for the first domain), as shown in Fig. 1, and after refinement we obtain that the AFM ordered transverse moment is $\mathcal{M}_X = 1.60(1)\mu_B$ per Cr^{3+} ion at $H = 6$ T. Considering the black atoms in this figure, *ferromagnetic* correlations between neighboring spins, i.e., *frustration*, are seen both within the (**a**, **b**) plane and between the planes. The field dependence (for $H < 6$ T) of the propagation wave-vector component $k = k_X = k_Y$ and that of $\mathcal{M}_X$ are displayed in Fig. 2 (open and solid circles). These data were from scans in the (110) direction across the strongest magnetic peak $(1 - k, 1 - k, 2)$ with $k \sim 0.25$, for increasing and decreasing magnetic field H. When increasing (decreasing) H, this peak could be detected from (down to) $H \sim 1.5$ T: H_{c1} is, then, slightly smaller than this value. Each scan was well fitted by a Gaussian function, giving rise to an accurate evaluation of both the integrated intensity, i.e., $\mathcal{M}_X^2$, and the wave-vector component k (see the inset of Fig. 2(a) where the magnetic peak is recorded for the same field value, $H = 2.9$ T, while H is increased or decreased). In $Cs_3Cr_2Br_9$, within the ordered phase, there are both incommensurabilities and large hysteresis effects suggesting pinning [10]. For increasing H, the commensurate $++--$ structure is reached at $H \sim 5$ T, while for decreasing H the commensurate structure remains locked down to $H \sim 3$ T. The *parallel* magnetization $\mathcal{M}_Z(H)$ was measured both by neutrons from the ferromagnetic contribution appearing on top of the weak nuclear Bragg peak (1, 1, 4) at $H = 6$ T [the open triangle in Fig. 2(b)] and from SQUID at $T \sim 100$ mK in the full field range (solid triangles).

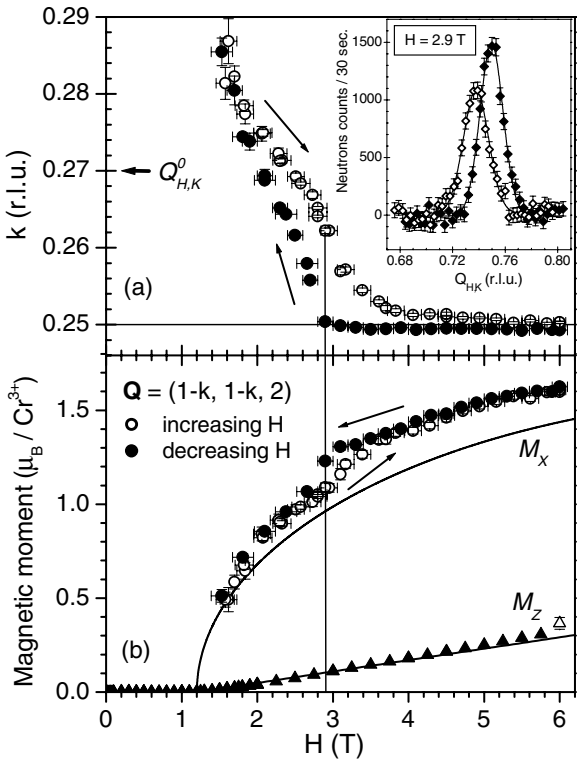

FIG. 2. (a) Field dependence of the propagation wave-vector component k ($= k_X = k_Y$) and (b) that of the parallel ($\mathcal{M}_Z$) and the ordered transverse ($\mathcal{M}_X$) magnetizations. $Q^o_{H,K}$ is the wave vector corresponding to the minima of the dispersions (see Fig. 3 and text). In (b) the solid lines are theoretical predictions obtained for the commensurate $++--$ magnetic order (see text).

Second, we report inelastic results. The same crystal was mounted on the cold neutron triple axis spectrometer IN12 FZ/CEA-CRG at ILL, in a 6 T vertical cryomagnet with a dilution insert. The measurements were performed in the same experimental configuration at $T \sim 50$ mK. The final wave vector $\mathbf{k}_f$ was fixed to various values between 1.07 and 1.55 Å^{-1}, depending on the explored energy range and the energy resolution that was needed. Examples of the dispersion as a

function of $Q_{H,K} = Q_H = Q_K$ (at $Q_L = 2$) are shown in Fig. 3.

For $H = 0$ (open squares), a unique excitation branch is observed, while three distinct branches are seen in the ordered phase (solid circles for $H = 3$ T). The description proposed in Ref. [5] for $H = 0$ reproduces very well the data (see solid line). From this fit, we obtain the following exchange values: $J = 1.03$ meV for the intradimer coupling, $J_p = 0.054$ and $J_c = 0.039$ meV for the in-plane and out-of-plane interdimer interactions, respectively, in agreement with Ref. [5]. We now focus on the minima of the dispersions, i.e., the three *energy gaps*. They always occur at the same wave-vector value $Q^o_{H,K} \sim 0.27$ r.l.u. (reciprocal lattice units), even above H_{c1} where the propagation vector component k varies continuously from 0.29 down to 0.25 r.l.u. [see Fig. 2(a)]. The field dependence of these gaps, obtained from energy scans performed at (0.27, 0.27, 2), is plotted in Fig. 4. The inset shows such a scan recorded at $H = 0$ with the best energy resolution ($k_f = 1.07$ Å^{-1}): a splitting, *not detected previously* [5], is clearly observed [11]. It reveals the presence of an additional anisotropy which can be described by a single-ion term $D(s_i^X)^2$ ($X \equiv \mathbf{c}$) at each Cr^{3+} site. Such a term results in a splitting of the initial dispersion. This effect can be accounted for by redefining for each branch two distinct effective intradimer couplings [7]: $J^- = J + 0.8D$ and $J^+ = J - 1.6D$ (for $s = 3/2$ and $D < 0$). From the splitting at the minimum of the dispersions, we evaluate $D \sim -0.01$ meV. With this value, the Zeeman splitting below H_{c1} (solid lines in Fig. 4) agrees also very well with the data. From the lowest energy branch, the critical field is expected at $H_{c1} \sim 1.5$ T, in agreement with the diffraction result. As mentioned above, for $H > H_{c1}$, three distinct branches are still observed. The two upper branches agree roughly with "Zeeman" behaviors: $g\mu_B H$ and $2g\mu_B H$ with $g = 2$ (dotted lines). The evidence for a gap ($\mathcal{E}_g$) on the lowest energy branch above H_{c1} is, however, a new result. It shows that there is no massless Goldstone mode in the FIMO phase of $Cs_3Cr_2Br_9$. In fact, even near H_{c1} the lowest energy gap does not vanish. The half-width (0.05 meV) of the fitted Gaussian at the minimum gap ~0.11 meV is instrumental.

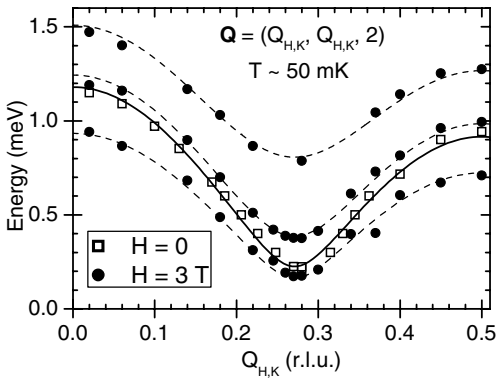

FIG. 3. Examples of dispersions for $H = 0$ and $H = 3$ T. The solid line for $H = 0$ is a fit as in Ref. [5]. The dashed lines for $H = 3$ T are guides to the eye.

Including the single-ion anisotropy D, the Hamiltonian for the spin dimers in $Cs_3Cr_2Br_9$ is

$$\mathcal{H} = \sum_i [J\mathbf{s}_{ia} \cdot \mathbf{s}_{ib} + D(s_{ia}^{X^2} + s_{ib}^{X^2}) - g\mu_B H(s_{ia}^Z + s_{ib}^Z)] + \sum_{i,m} J'(\mathbf{s}_{ia} \cdot \mathbf{s}_{ma} + \mathbf{s}_{ib} \cdot \mathbf{s}_{mb}), \quad (1)$$

with $J' = J_p$ (J_c) for in- (out-of-)plane couplings. In Eq. (1), the indices a and b refer to the two spins in each dimer while the index m accounts for the interacting spins surrounding each spin i (six in-plane and 2×3 out-of-plane couplings). Because of the spin value $s = 3/2$, three distinct plateaus are, *a priori*, expected in the magnetization curve of such a compound. They are actually observed in the parent compound $Cs_3Cr_2Cl_9$, and magnetic ordered phases are expected to precede each of the three plateaus [12]. The situation is different in $Cs_3Cr_2Br_9$, where the magnetization constantly increases from $H_{c1} \sim 1.3$ T up to saturation ($H_s \sim 26$ T) without intermediate plateaus [12]. This means that the three FIMO phases in this compound overlap, giving rise to a single FIMO phase, hereafter called the *extended* FIMO phase. In general, a *simple* FIMO phase develops each time a crossing occurs between two states of the isolated dimers. In low field, $H \sim H_{c1}$, the crossing occurs between the singlet ground state $|0\rangle$ and the lowest Zeeman split state $|1, -1\rangle$ (including anisotropy) of the initial triplet state $|1\rangle$. For a simple FIMO phase, an effective Hamiltonian $\mathcal{H}_{\text{eff}}$ can be derived by projecting Eq. (1) onto these elementary states. One obtains a $\sigma = \frac{1}{2}$ pseudospin Hamiltonian, which, for the initial $s = 3/2$

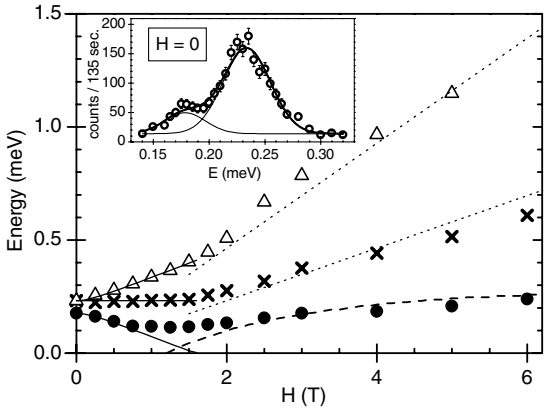

FIG. 4. Field dependence of the energy gaps. The solid lines describe the splitting below H_{c1}. Above H_{c1}, the dotted lines are $g\mu_B H$ and $2g\mu_B H$. The dashed line describes the lowest gap $\mathcal{E}_g$ (see text). Inset: $H = 0$ energy scan performed at (0.27, 0.27, 2) with $k_f = 1.07$ Å^{-1}. The splitting signals the presence of a small single-ion anisotropy [D in Eq. (1)]. The slightly broader width of the upper mode indicates the possible presence of small higher-order anisotropies.

spin system, is given to first order as

$$\mathcal{H}_{\text{eff}} = \sum_{i,m} J^{XY}_{\text{eff}}(\sigma^X_i\sigma^X_m + \sigma^Y_i\sigma^Y_m) + J^Y_{\text{eff}}\sigma^Z_i\sigma^Z_m + d_{\text{eff}}(\sigma^X_i\sigma^X_m - \sigma^Y_i\sigma^Y_m) - \sum_i g\mu_B H_{\text{eff}}\sigma^Z_i, \quad (2)$$

with $J^{XY}_{\text{eff}} = 2M^2J'$, $J^Z_{\text{eff}} = J'(c_1^2 - c_{-1}^2)^2/2$, $d_{\text{eff}} = -4M^2J'c_1c_{-1}$, and $g\mu_B H_{\text{eff}} = g\mu_B H(c_1^2 - c_{-1}^2) + J + J'(c_1^2 - c_{-1}^2)/4 - R^2D$. In these expressions, $M = {}^o\langle 1,-1|s_X|0\rangle = -\sqrt{5/2}$, $R = -2(1 - 6c_1c_{-1})/5$, c_1 and c_{-1} account for the mixing of the initial states (no anisotropy): $|1,-1\rangle = c_{-1}|1,-1\rangle^o + c_1|1,1\rangle^o$, with $c_{-1} = \beta D/[(\beta D)^2 + \{[(g\mu_B H)^2 + (\beta D)^2]^{1/2} - g\mu_B H\}^2]^{1/2}$ and $c_1 = \{[(g\mu_B H)^2 + (\beta D)^2]^{1/2} - g\mu_B H\}/[(\beta D)^2 + \{[(g\mu_B H)^2 + (\beta D)^2]^{1/2} - g\mu_B H\}^2]^{1/2}$, where $\beta = 2^o\langle 1,-1|s_X^2|1,+1\rangle^o = 6/5$. We note that the ratio $J^Z_{\text{eff}}/J^{XY}_{\text{eff}} \sim 1/(4M^2) = 1/10$ is much smaller than in the $s = 1/2$ spin case [13]; i.e., for $s = 3/2$, the pseudospin Hamiltonian is almost XY. More novel is the XY anisotropy term d_{eff}. This anisotropy is induced by D, but it occurs indirectly through the mixing coefficient c_1c_{-1}. Note that higher-order anisotropies within the YZ hexagonal plane (see Fig. 4 caption) would renormalize slightly the ratio $J^Z_{\text{eff}}/J^{XY}_{\text{eff}}$ and d_{eff}, but otherwise does not affect the analysis. According to Eq. (2), in a simple FIMO phase, one has an anisotropic quantum pseudospin 1/2 XYZ model. For an extended FIMO phase, as in $Cs_3Cr_2Br_9$, the pseudospin description should give the essential physics, but one expects deviations. We now compare our data and predictions from Eq. (2). For the σ spin system, we analyze the commensurate $++--$ structure of the FIMO phase. The effective couplings in the mean-field approximation according to the spin arrangement displayed in Fig. 1 (see the black atoms) are $\langle J^{XY}_{\text{eff}}\rangle = -4(J_p + J_c/2)M^2$ and $\langle d_{\text{eff}}\rangle = +4(J_p + J_c/2)M^2c_1c_{-1}$. The calculated $\mathcal{M}_Z$ and $\mathcal{M}_X$, with $\mathcal{M}_X = 2|M|\sqrt{\mathcal{M}_Z(1 - \mathcal{M}_Z)}$, are represented by the solid lines in Fig. 2(b). The observed behaviors are well explained qualitatively. Quantitatively, at $H = 6$ T, the discrepancy between measurements and this simple theory is $\sim$15% for $\mathcal{M}_X$. Such a correction is what one expects when one compares the results for a simple and an extended FIMO, i.e., when the contributions from the higher states are taken into account [14]. Extrapolation of these curves to lower fields predicts a reasonable critical value, $H_{c1} \sim 1.2$ T.

A FIMO corresponds to an *AFM spin-flop* state. A small anisotropy, such as d_{eff} in Eq. (2), breaks the axial symmetry responsible for the Goldstone mode and opens a gap in the XY fluctuations. By Holstein-Primakoff transformation on the pseudospin Hamiltonian, extending the standard treatment [15] to include d_{eff}, gives

$$\mathcal{E}_g \sim 4\sigma_X^2\sqrt{\langle J^{XY}_{\text{eff}}\rangle\langle d_{\text{eff}}\rangle} = 16\sigma_X^2(J_p + J_c/2)M^2\sqrt{|c_1c_{-1}|}, \quad (3)$$

where $\sigma_X = \mathcal{M}_X/(2|M|)$ is the ordered transverse component of the $\sigma = 1/2$ spins ($0 < \sigma_x < \sigma = 1/2$). The prediction from Eq. (3) applies to a simple FIMO. In the case of an extended FIMO, one expects additional contributions resulting from the mixing of states. An "amplification" factor is therefore to be expected. As shown by the dashed line in Fig. 4, with a multiplying factor $\sim$5, Eq. (3) provides a quite good agreement with the data. This factor is surprisingly large and suggests that the dynamics is much more sensitive to the extended nature of the FIMO than the statics.

At $H = H_{c1}$, a FIMO transition is expected to be of second order. The transition here is complicated by the frustration: the magnons that soften are incommensurate and degenerate in momentum space [5]. The initial ordering vector appears away in wave-vector space from the minimum gap, which, remarkably, remains nonzero at the transition. The complexity seen in our results as to the evolution of the ordering vector towards a locked-in commensurate value with collinear spins, is, we believe, due to interplay of quantum fluctuations, enhanced by the frustration of the hexagonal lattice and the anisotropy. Even in the commensurate phase a small anisotropy, since it opens a gap, changes the nature of the magnon condensation.

We have observed new and peculiar features at the onset of field-induced magnetic order in $Cs_3Cr_2Br_9$. They should stimulate new developments concerning simple versus extended FIMO, incommensurability, and hysteretic behavior.

We thank E. Ressouche and J. Rodriguez Carvajal for help in the structural refinement.

[1] I. Affleck, Phys. Rev. B **43**, 3215 (1991).
[2] T. Nikuni *et al.*, Phys. Rev. Lett. **84**, 5868 (2000).
[3] Ch. Rüegg *et al.*, Nature (London) **423**, 62 (2003).
[4] T. Kato *et al.*, J. Phys. Soc. Jpn. **67**, 752 (1998).
[5] B. Leuenberger *et al.*, Phys. Rev. B **30**, 6300 (1984).
[6] B. Leuenberger *et al.*, Phys. Rev. B **31**, 597 (1985). Note $H_{c1} \sim 1.5$ T is smaller than the value in that reference. This is an effect of temperature (see Ref. [7]).
[7] B. Leuenberger, J. Phys. C **19**, 4083 (1986).
[8] B. Leuenberger *et al.*, J. Solid State Chem. **64**, 90 (1986).
[9] Throughout the text, the wave vectors are expressed in reciprocal lattice units (r.l.u).
[10] W. L. McMillan, Phys. Rev. B **14**, 1496 (1976).
[11] In Fig. 3, the data for $H = 0$ were obtained with $k_f = 1.25$ Å^{-1}; the splitting of each mode could not be seen.
[12] Y. Inagaki, Ph.D. thesis, Kyushu University, Fukuoka, Japan, 2003. In $Cs_3Cr_2Cl_9$, $H_{c1} \sim 12$ T. This precludes a full (statics and dynamics) study by neutrons.
[13] M. Tachiki *et al.*, J. Phys. Soc. Jpn. **28**, 1413 (1970).
[14] T. Ziman *et al.* (unpublished).
[15] B. R. Cooper *et al.*, Phys. Rev. **127**, 57 (1962).